Taxol–Lipid Interactions: Taxol-Dependent Effects on the Physical Properties of Model Membranes†

Sathyamangalam V. Balasubramanian and Robert M. Straubinger*

Department of Pharmaceutics, University at Buffalo, State University of New York, Amherst, New York 14260-1200

Received December 8, 1993; Revised Manuscript Received May 10, 1994®

ABSTRACT: Taxol (paclitaxel) is a diterpenoid anticancer agent undergoing intensive human clinical evaluation. The poor aqueous solubility of taxol necessitates administration in excipients causing a variety of adverse effects, including anaphylactoid hypersensitivity reactions. Recently, taxol has been formulated in better-tolerated drug carriers such as liposomes. We investigated the conformation of taxol and the interaction of taxol with dipalmitoylphosphatidylcholine (DPPC) liposomes using fluorescence, circular dichroism, differential scanning calorimetry, fluorescence polarization, and X-ray diffraction. The conformation of taxol in DPPC membranes was similar to that observed in nonpolar solvents such as chloroform. Taxol was found to partition into the bilayer, perturbing the hydrocarbon chain conformation. The taxol C13 side chain was found to be fluorescent, and it displays an environment-sensitive shift in emission spectrum; taxol fluorescence was used to confirm the insertion of the drug into the bilayer. Taxol induces a broadening of the DPPC phase transition, and the location of the drug in the bilayer depends on drug concentration. Incorporation of taxol affects other physical properties of the bilayer such as the lipid order parameter, and this fluidizing effect was also observed upon incorporation of taxol in biological membranes isolated from basolateral plasma membranes of rat liver. These studies demonstrate that taxol incorporated into liposomes penetrates into the acyl chain domain of the bilayer and alters the physical properties of both artificial and biological membranes.

Taxol is a complex diterpenoid natural product of the western yew, *Taxus brevifolia* (Wani, et al., 1971) (Figure 1), and is under investigation in phase I, II, and III human clinical trials for treatment of various human cancers, including colon, ovarian, lung, and breast cancer, as well as melanoma and lymphoma (Donehower et al., 1987; Grem et al., 1987; Rowinsky et al., 1990). However, clinical development has been hampered by the poor aqueous solubility of taxol, which necessitates administration of the drug in a vehicle of polyethoxylated castor oil (Cremophor EL) and 50% ethanol. Unfortunately, both the drug and its formulation vehicle have been observed to cause toxicity (Donehower et al., 1987; Lorentz, et al., 1977).

Liposomes (phospholipid vesicles) have been used to formulate a variety of hydrophobic, poorly soluble drugs (Popescu et al., 1987; Szoka, 1991). Presently we are developing liposome-based formulations for improved solubilization of taxol (Sharma et al., 1993; Sharma & Straubinger, 1994; Straubinger et al., 1993); these formulations avoid the acute toxicity associated with administration of drug in the conventional ethanol/polyethoxylated castor oil (Cremophor EL) vehicle and show reduced chronic taxol toxicity as well (Sharma et al., 1993; Sharma & Straubinger, 1994; Straubinger et al., 1993). Antitumor effects in a taxol-resistant murine model system were observed to be greater than those of the clinically used taxol formulation, suggesting that the incorporation of taxol in drug carriers such as liposomes may provide additional therapeutic gains.

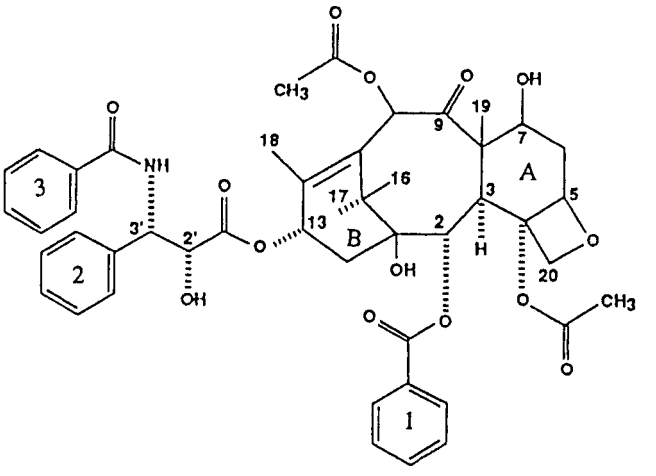

FIGURE 1: Chemical structure of taxol.

It has been shown that a variety of cytostatic drugs interact strongly with the phospholipid components of cellular bilayer membranes, and it is believed that drug–membrane interactions play a role in the cytotoxicity of several anticancer agents (Canaves et al., 1991; Deliconstantonos et al., 1987; Wright & White, 1986). However, taxol interaction with membranes has not been investigated in detail, and such interactions may lend insight not only into the therapeutic performance of taxol–liposome formulations but also into other novel mechanisms of action and cellular effects of taxol (Brugg & Matus, 1991; Ding et al., 1990).

Recent studies of taxol conformation in a variety of solvent systems suggest that the molecule is sensitive to the environment (Vander Velde et al., 1993) and that the drug has a tendency to undergo self-aggregation (Balasubramanian et al., 1994). Here we extend those studies to examine the interaction of taxol with phospholipid membrane bilayers and the physical state of taxol within liposome drug carriers.

† Supported by Grant CA55251 from the National Cancer Institute, National Institutes of Health.

* Corresponding author: Department of Pharmaceutics, 539 Cooke Hall, University at Buffalo, State University of New York, Amherst, NY 14260-1200. Telephone: (716) 645-2844. FAX: (716) 645-3693. Internet: rms@acsu.buffalo.edu.

® Abstract published in *Advance ACS Abstracts,* July 1, 1994.

0006-2960/94/0433-8941$04.50/0

Experiments were designed to investigate the location and conformation of taxol in dipalmitoylphosphatidylcholine (DPPC)[1] liposomes by means of fluorescence, circular dichroism (CD), differential scanning calorimetry (DSC), fluorescence polarization (using diphenylhexatriene as a probe), and X-ray diffraction.

EXPERIMENTAL PROCEDURES

DPPC was obtained from Avanti Polar Lipids as a chloroform solution and was stored at −70 °C. Solvents were of spectroscopic grade from Fisher Scientific and were used without further purification. Taxol was obtained from the National Cancer Institute and used without further purification. It eluted as a single peak when assayed by HPLC, using a reverse-phase C18 column (Waters μBondapak, 3.9 × 300 mm, 10-μm particle size) and a mobile phase of methanol:water (70:30), and was detected at 227 or 280 nm (data not shown). The HPLC equipment used was from Hitachi (Danbury, CT) and consisted of an L6200A pump, an AS-2000 automated injector equipped with a 100-μL loop, an L-4250 UV–vis detector, a D-2500 integrator, and an F1080 scanning fluorescence detector. NMR spectra of taxol taken in solvents of varying polarity further confirmed the purity of the drug (Balasubramanian et al., 1994). Diphenylhexatriene (DPH) was obtained from Molecular Probes, Inc..

Preparation of Liposomal Dispersions. Multilamellar vesicles (MLV) were used for DSC and X-ray studies, and small unilamellar vesicles (SUV) were used for optical measurements (CD and fluorescence) to reduce light-scattering effects. The required amount of DPPC was dissolved in chloroform, and the solvent was removed using a rotary evaporator, depositing the lipid as a thin film on the walls of a round-bottomed flask. In cases where taxol was incorporated, the drug was dissolved in chloroform and the desired amount was added to the chloroform–lipid solution before solvent removal. The lipid film was dispersed in aqueous medium at 50 °C and vortexed vigorously. The resulting MLV were sonicated with a bath-type sonicator (Laboratory Systems, Inc.) to obtain SUV.

Preparation of Basolateral Membranes. Basolateral plasma membrane vesicles were prepared from rat liver using self-generating Percoll gradients (Blitzer & Donovan, 1984). The protein concentration was measured using a micro protein determination kit (Sigma Chemical Co., St. Louis), using bovine serum albumin as a standard. The final protein concentration in assays was 0.1 mg/mL, and the vesicles thus prepared did not pose any problem with light scattering during the polarization measurements.

CD Studies. CD studies were performed on a Jasco 600 machine interfaced to an IBM PS/2 microcomputer and calibrated with d_{10}-camphorsulfonic acid. The path length of the quartz cuvette used was 1 mm, and SUV were used in order to reduce the effects of light scattering.

Fluorescence Studies. Emission spectra of taxol were taken using an SLM Aminco 8000 series machine. Samples were excited at 270 nm, with 4-nm excitation and emission slits. Fluorescence polarization measurements were made using FP110 film polarizers from SLM. Fluorescence polarization was calculated as reported elsewhere (Sarkar et al., 1993), using diphenylhexatriene (DPH) as a probe. Samples containing DPH were excited at 355 nm, and the emission was monitored at 430 nm, using 4-nm excitation and emission slits. To incorporate DPH into liposomes, a stock of 2 mM DPH was prepared in tetrahydrofuran, and 2 μL was added to 2 mL of a liposome suspension containing 0.6 mM phospholipid. The suspension was mixed by rapid vortexing above the phase transition temperature (T_m) (Lentz et al., 1976). For biological membranes, probe incorporation was carried out at 37 °C. During the fluorescence measurements, the cuvette chamber was maintained at the required temperature using a Neslab (RTE 110) circulating water bath. Temperature equilibration was established by maintaining the chamber at the appropriate temperature for 15 min prior to the measurements. Corrections for light scattering were applied by performing appropriate control experiments without added probe, as described previously (Shinitzky & Barenholz, 1978; Shinitzky et al., 1971). The lipid order parameter (S) was calculated from the steady state anisotropy value by the following relationship: $S^2 = \{(4r/3) - 0.1\}/r_0$, where r_0 is the maximal fluorescence anisotropy value in the absence of any rotational motion (taken as 0.40), and r is the steady-state anisotropy (Pottel et al., 1983).

X-ray Diffraction Studies. X-ray diffraction data were recorded using the film method, with Cu K radiation (λ = 1.5418 Å) from a rotating-anode X-ray generator. The samples were sealed in thin-walled capillary tubes and mounted in sample holders maintained at 25 °C. The exposure time was typically 10–15 min.

DSC Studies. Calorimetry was performed using a Perkin-Elmer DSC-2 instrument with samples sealed in aluminum pans. The instrument was calibrated with standard samples covering a wide range of temperatures. Thermograms were recorded using a heating rate of 2.5 K/min and a range of 1 mcal/sec. For each thermogram, 14 μL of a 55 mM liposome suspension was used. Samples were kept at the initial temperature (25 °C) for 15 min before each experiment.

RESULTS AND DISCUSSION

Insertion and Conformation of Taxol in DPPC Vesicles

Fluorescence Studies. We observed that taxol is fluorescent, with an excitation maximum at 270 nm; the emission maximum was observed in the range of 310–350 nm, depending on the solvent. Figure 2 shows emission spectra obtained for 10^{-5} M taxol in various solvents. Taxol was resolved chromatographically by HPLC, using both UV and fluorescence detectors, to determine whether the fluorescence is a property of taxol or of a copurified contaminant. The UV detector was set at 227 nm, the peak absorbance of taxol, and the fluorescence detector was set with the excitation at 270 nm and the emission at 312 nm. A 295-nm long-pass filter was included on the emission side of the optical path to reduce scattered excitation light. Taxol eluted with a retention time of 7.4 min, as observed by UV absorbance; the peak appeared on the fluorescence detector after the appropriate delay introduced by the length of tubing between the two detectors (data not shown).

The fluorescence of taxol likely arises from the C13 side chain (numbered as in Figure 1), in which two aromatic groups are connected through a peptide-like bond. Taxotere, a semisynthetic analog of taxol in which the aromatic ring 3 of the C13 side chain is replaced by an *O-tert*-butyl group, likewise is fluorescent (data not shown), suggesting that both aromatic groups are not essential for fluorescence. However, the molar fluorescence of taxotere is lower than that of taxol, implying that two aromatic groups contribute to an enhanced quantum yield.

[1] Abbreviations: DPPC, dipalmitoylphosphatidylcholine; DPH, 1,6-diphenyl-1,3,5-hexatriene; UV, ultraviolet; CD, circular dichroism; DSC, differential scanning calorimetry; BLM, basolateral membrane; MLV, multilamellar vesicles; SUV, small unilamellar vesicles; T_m, bilayer phase transition temperature.

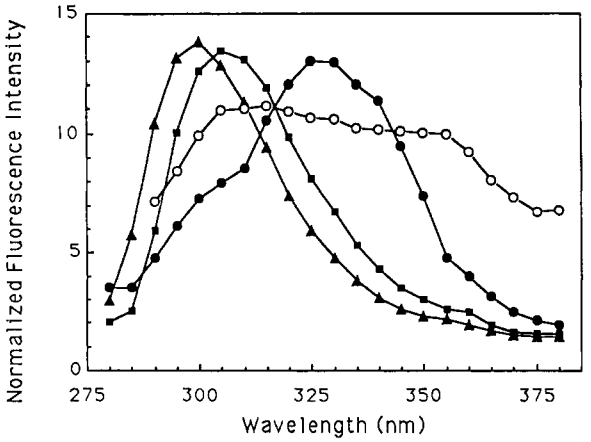

FIGURE 2: Environment-sensitive fluorescence emission spectra of taxol. Fluorescence emission spectra of 10^{-5} M taxol were acquired in solvents of varying polarity or in dipalmitoylphosphatidylcholine liposomes. Taxol samples in solvent were excited at 270 nm, with 4-nm excitation and emission slits, and the temperature was held at 20 °C. Taxol in DPPC vesicles was excited at 260 nm, with 4-nm excitation and emission slits; the temperature was held at 50 °C, and the lipid concentration was 0.6 mM. The highest intensity was observed for taxol in methanol; all other spectra were rescaled so that peak values are comparable to the height of that for taxol in methanol. Filled triangles, acetonitrile; filled squares, chloroform; filled circles, methanol; open circles, sonicated DPPC liposomes.

The taxol emission spectrum was found to be highly dependent upon solvent polarity (Figure 2). Replacement of chloroform by more polar solvents such as methanol resulted in a shift of the emission maximum toward longer wavelengths. The observed dependence of the spectral characteristics of taxol upon solvent are consistent with a fluorophore–solvent interaction.

The environment-sensitive fluorescence emission was used to investigate taxol insertion into bilayer membrane vesicles of dipalmitoylphosphatidylcholine. Taxol was added to preformed, sonicated DPPC liposomes to a final concentration of 10^{-5} M, corresponding to a drug:lipid ratio of 1:60. The observed emission maximum of taxol was red-shifted relative to the spectrum obtained in polar solvents such as methanol (Figure 2) or water (not shown), suggesting that taxol partitions into a less polar environment, such as the interior of the bilayer.

The aqueous concentration of taxol used in experiments with liposomes (10^{-5} M) equals or exceeds the solubility limit in pure water, for which estimates range from 0.77 (Mathew et al., 1992) to 35 μM (Ringel & Horwitz, 1991; Swindell & Krauss, 1991). To ascertain whether the fluorescence signal arose from taxol incorporated in liposomes, rather than from precipitated drug, samples were examined by optical microscopy using phase contrast optics. Taxol precipitates were not observed, suggesting incorporation of a majority of the drug into liposomes (observations similar to the experiments described in Figure 6d–f). Partitioning of taxol into the phospholipid bilayer would be anticipated qualitatively from the structure of the molecule (Figure 1) and from the analysis of the fractional lipophilicity of taxol probed by aromatic solvent induced chemical shift analysis (ASIS) (Balasubramanian et al., 1994). Incorporation of taxol into the lipophilic domain of membranes was estimated quantitatively by calculating the partition coefficient (K) in three different bulk solvent:water systems employing hexane, ether, or butanol. The partitioning of taxol in any of the solvent systems exceeded 96%. The K values derived using UV absorbance data are comparable to those reported for highly hydrophobic molecules (Diamond & Katz, 1974); the data and methods for determining taxol partition coefficients will be reported elsewhere.

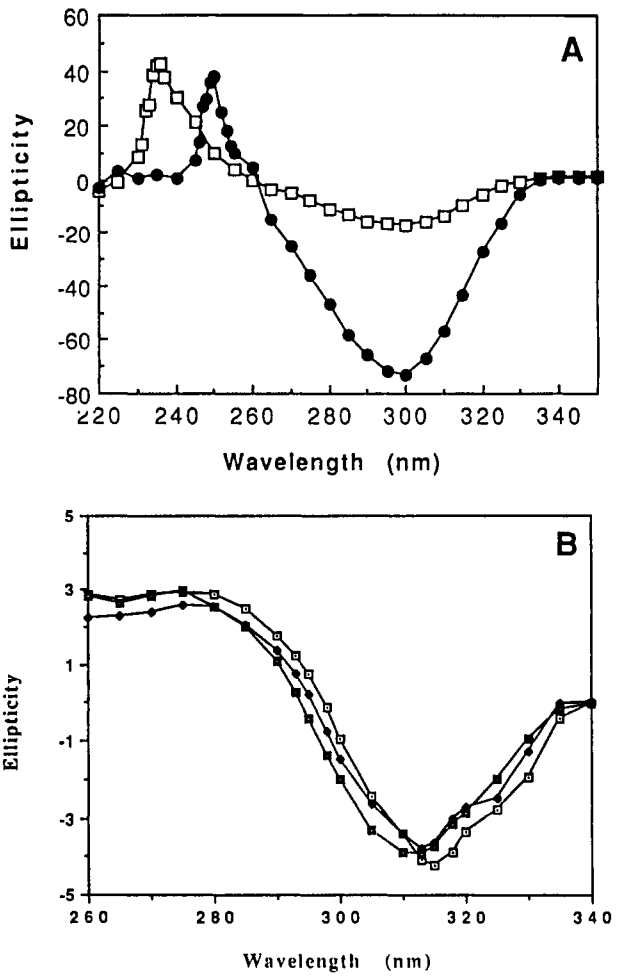

FIGURE 3: Concentration- and solvent-dependent CD spectra. (A) CD spectra acquired over the range of 220–360 nm for two different concentrations of taxol in chloroform. Filled circles, 10^{-3} M taxol; open squares, 10^{-4} M taxol. (B) First-derivative CD spectra acquired over the range of 260–340 nm for taxol at a concentration of 10^{-4} M in solvents of varying polarity. Open squares, taxol in chloroform; filled squares, taxol in methanol; filled circles, taxol in acetonitrile.

Other observations supporting the insertion of taxol into domains of DPPC was obtained from measurements of the pressure–area curves for binary taxol:DPPC monolayers, measured using a Langmuir balance; such measurements showed the complete miscibility of taxol in DPPC at drug:lipid ratios ≤ 2.[2]

Taxol Conformation in Bilayer Membranes

Conformation and Aggregation of Taxol Dependent on Solvent. Previously we observed that taxol exhibits a strong Cotton effect and that taxol shows both solvent- (Balasubramanian et al., 1994) and concentration-dependent changes that are readily detectable by circular dichroism. The CD spectrum of taxol in chloroform (10^{-4} M) has two prominent bands: one broad negative band at 298 nm having a shoulder at 264 nm, and a positive band at 232 nm (Figure 3A). A more comprehensive study of taxol solution conformation by CD and NMR (Balasubramanian et al., 1994) suggests the following assignments: the band at 298 nm is due to the π–π^* transition of the aromatic rings in the taxol side chain, and the 264 nm shoulder may be due to the C2–O–benzoyl group. The 232-nm band corresponds to n–π^* transitions involving two C=O groups, one at C9 and the other from the peptide-like bond in the C13 side chain.

[2] S. V. Balasubramanian, D. M. Leckband, and R. M. Straubinger, unpublished data.

The broad negative CD band shifts to shorter wavelengths with increases in solvent polarity. For 10^{-4} M taxol in methanol, the peak was observed at 294 nm. Figure 3B compares the 1st-derivative CD spectrum of taxol in methanol with those obtained in chloroform or acetonitrile [data from Balasubramanian et al. (1994)], demonstrating that the spectral shift is dependent on solvent polarity.

Detailed NMR studies on the solution conformation of taxol in nonpolar solvents (Baker, 1992; Balasubramanian et al., 1994; Chmurny et al., 1992; Falzone et al., 1992; Kingston et al., 1982; Vander Velde et al., 1993) and in polar solvent systems such as DMSO-d_6/water (Vander Velde et al., 1993; Williams et al., 1993) can be used to give further insight into the conformational changes that lead to the observed changes in the CD spectrum. These studies indicate that the conformation of the C13 side chain is highly sensitive to the polarity of the solvent. The coupling constant JH2′–H3′ changes from 8 Hz in water to 2.6 Hz in $CDCl_3$, and the change is interpreted as a polarity-dependent rotation around C2′–C3′. Because of the location of the side-chain chromophore, side-chain conformational changes observed by NMR would be expected to correlate with the solvent-dependent shift observed in the CD spectrum (Balasubramanian et al., 1994).

The CD spectrum of taxol is not only solvent-dependent but also concentration-dependent. The spectra for two different concentrations of taxol in chloroform are shown in Figure 3A. With an increase in taxol concentration to 10^{-3} M, the positive band observed at 232 nm (for 10^{-4} M taxol) shifts to a longer wavelength (~245 nm). Similar CD spectral changes were observed for taxol in acetonitrile. On the basis of the solvent-, temperature-, and concentration-dependent effects observed by NMR (Balasubramanian et al., 1994), the shift in the 232-nm peak is ascribed to taxol aggregation involving the four exchangeable protons (1-OH, 7-OH, 2′-OH, and 3′-NH).

On the basis of the conformational studies of taxol in organic solvents, the following conclusions are drawn: (i) The appearance of a local maximum at 245 nm (via a shift of the 232-nm band to longer wavelengths) marks the aggregation of taxol. (ii) The shift of the broad >290-nm negative band toward longer wavelengths indicates localization of taxol in a nonpolar environment and is correlated with a C2′–C3′ bond rotation in the C13 side chain.

Conformation and Aggregation of Taxol in Membranes. The CD spectrum of 10^{-6} M taxol in water (Figure 4A) shows two prominent bands: one broad negative band around 294 nm and a positive band at 232 nm. Upon the external addition of DPPC vesicles to a final drug:lipid ratio of 1:450 (at $T > T_m$ for the bilayer phase transition), the negative CD band shifts toward longer wavelengths, suggesting a conformational change that occurs in the C13 side chain (rotation around C2′–C3′) upon transfer of taxol from water to a less polar environment. Such observations reinforce qualitatively the conclusions based on fluorescence spectroscopic observations (discussed above) regarding the intramembrane environment of taxol.

In order to investigate the physical state of membrane-associated taxol at the higher drug:lipid ratios comparable to those of taxol:liposome formulations used in therapeutic experiments (Sharma et al., 1993; Sharma & Straubinger, 1994; Straubinger et al., 1993), CD spectra were acquired for suspensions containing taxol at 1 mol % (with respect to phospholipid). As shown in Figure 4B, a small negative band was observed at 245 nm, in addition to a large positive band at 232 nm and a broad negative band at >290 nm. The

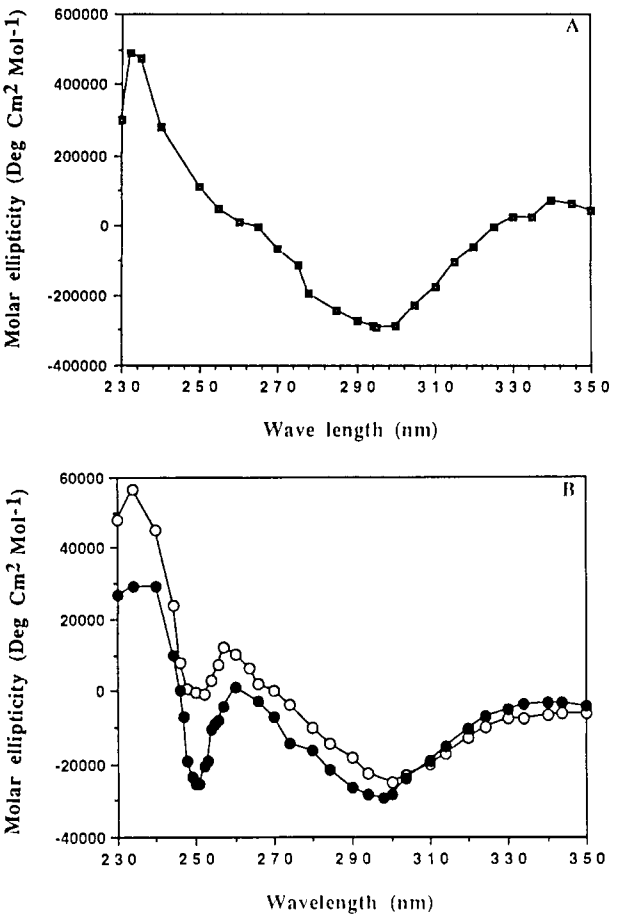

FIGURE 4: CD spectra of taxol in water or in phospholipid vesicles. (A) CD spectrum of taxol in water over the range of 230–350 nm. The concentration of taxol (10^{-6} M) was near its limit of aqueous solubility. (B) CD spectra of taxol incorporated at varying drug:lipid ratios in sonicated DPPC liposomes. The temperature was held at 20 °C. Open circles, 1 mol % taxol; the bulk taxol concentration was 0.22 mM. Filled circles, 2.8 mol % taxol; the bulk taxol concentration was 0.67 mM.

spectrum for 1 mol % taxol in liposomes (Figure 4B) is similar to that of 10^{-3} M free taxol in chloroform (cf. Figure 3A), but with several differences. First, the positive band observed near 245 nm in chloroform appears as a negative band for taxol in DPPC liposomes. Second, the curve shoulder observed at 264 nm in chloroform is resolved into a positive band upon incorporation of taxol into DPPC vesicles. Changes in the 245- and 264-nm bands occurring in the presence of liposomes were more pronounced at higher taxol:lipid ratios (cf. Figure 4B; described below).

The observation of the 245-nm band in 10^{-3} M taxol in chloroform (Figure 3A) was interpreted as evidence of concentration-dependent taxol aggregation; the observation of a similar band in taxol–liposome suspensions likewise suggests the presence of drug aggregates in the membrane. A comparison of the intensities of the bands at 245 and 232 nm suggests the predominance of monomer taxol over aggregates. Further, the position of the broad negative band indicates a nonpolar location of the drug and suggests that the drug remains localized in the bilayer. Thus at lower drug:lipid ratios, monomer taxol exists together with a minor population of aggregated drug.

In order to investigate events that occur as the taxol:lipid ratio approaches the membrane capacity for stable drug incorporation in liposomes (Sharma & Straubinger, 1994), CD spectra were taken for liposome suspensions in which taxol was incorporated at 2.8 mol % (with respect to the

phospholipid) (Figure 4B). Compared to the CD spectrum of a 1 mol % taxol:lipid ratio, 2.8 mol % taxol showed a more intense negative band at 245 nm and a less intense positive band at 232 nm, interpreted as evidence for a further increase in the fraction of aggregated taxol and a reduction in monomer taxol. Changes in the 264-nm band that were small with 1 mol % taxol became more distinct at 2.8 mol % taxol:lipid, suggesting that the partitioning of taxol into DPPC bilayers results in conformational changes that may involve groups in the C2–O–benzoyl region (aromatic ring 1), in addition to those discussed above for the C13 side chain. The conformational changes in the C2–O–benzoyl group may result from the hydrophobic environment of the group upon incorporation into the membrane. It was observed by Vander Velde et al. (1993) that during the hydrophobic clustering of taxol in aqueous and mixed solvent systems the C2–O–benzoyl group becomes spatially closer to the hydrophobic C3′ phenyl ring. The CD spectra presented here for taxol in DPPC liposomes suggest that conformational changes are observed in the C2–O–benzoyl group, in addition to changes in the taxol side chain, due to the hydrophobic environment provided by the membrane. Incorporation of taxol into membranes results in the aggregation of taxol in a manner similar to that observed previously (Balasubramanian et al., 1994) in nonpolar solvents such as chloroform and acetonitrile. Furthermore, a comparison of the CD spectra obtained at successively higher drug:lipid ratios suggests a further aggregation of taxol, with the aggregated form predominating over the monomer form in DPPC liposomes containing ≥2.8 mol % taxol.

We observed previously that at higher drug:lipid ratios taxol precipitates out of therapeutic liposome formulations as needlelike crystals in the aqueous medium (Sharma & Straubinger, 1994; Straubinger et al., 1993). Since the CD spectrum of taxol in water is distinct from that of taxol in liposomes, and because aggregated taxol has distinct CD spectral characteristics, CD spectroscopy may provide a rapid and sensitive method to evaluate the stability of taxol–liposome formulations during development, production, or storage.

Effect of Taxol on DPPC Bilayer Physical State. Owing to the presence of two aromatic rings (Figure 1), the side chain of taxol is expected to be more hydrophobic than the main taxane ring. Such an assumption was confirmed by previous NMR studies using aromatic solvent induced chemical shift values (ASIS) (Balasubramanian et al., 1994). The influence of taxol structure on the location of the drug in the bilayer might have an impact on the stability of taxol–liposome formulations and also on drug interactions with biological membranes. Differential scanning calorimetry, X-ray diffraction, and fluorescence polarization studies were carried out to determine the location of the drug in the bilayer and its possible effect on the phospholipid hydrocarbon chain conformation.

Fluorescence Polarization Studies. Diphenylhexatriene (DPH) was used to investigate the structural order of the acyl chain portion of the bilayer, because the location of the probe in the hydrophobic matrix has been well studied. The fluorescence polarization of DPH is sensitive to the fluidity of liposomes (Lentz et al., 1976; Shinitzky & Barenholz, 1978; Shinitzky et al., 1971), and it decreases at $T > T_m$ because of the increased rotational freedom of the probe upon melting of the phospholipid acyl chains. The fluorescence polarization of DPH in DPPC vesicles was monitored as a function of both taxol concentration in the bilayer and temperature (in the range of the T_m of the liposomes), in order to study the structural order of the lipid bilayer core. Taxol decreases the polarization of DPH in a concentration-dependent fashion

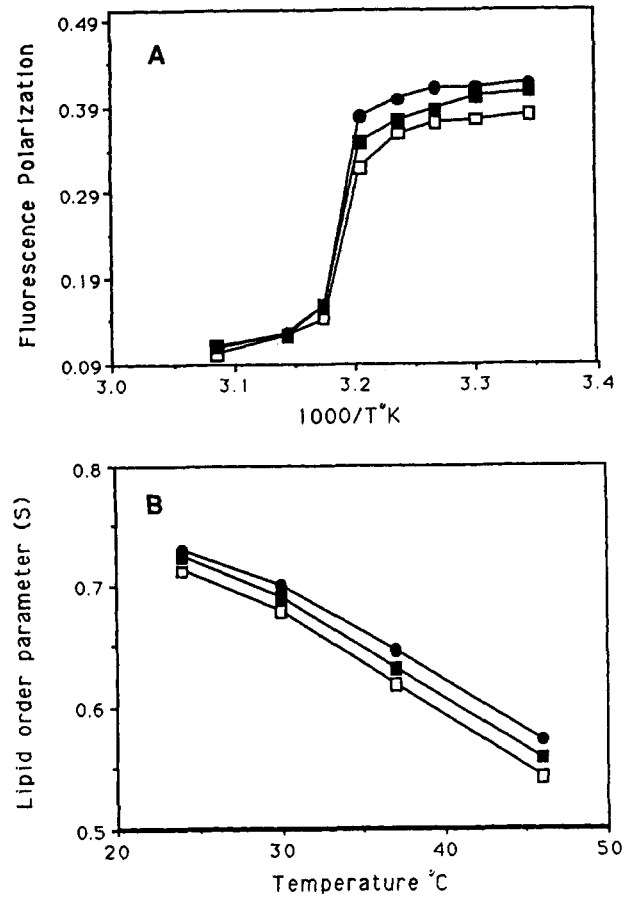

FIGURE 5: Taxol-dependent effects on membrane-incorporated diphenylhexatriene fluorescence polarization. Sonicated liposomes of DPPC or biological membranes isolated from liver basolateral membranes (BLM) were incubated in the presence of 2 μM DPH, added from an ethanolic stock solution. The final concentration of ethanol was 0.1%. DPPC liposomes were incubated with probe at 45 °C, and BLM were incubated at 37 °C. Samples were excited at 355 nm, and the emission was monitored at 430 nm, using 4-nm excitation and emission slits. Fluorescence polarization was measured as a function of temperature and taxol concentration. (A) Fluorescence polarization of DPH in DPPC liposomes. The lipid concentration was 0.6 mM. Filled circles, DPPC liposomes without taxol; filled squares, 0.8 mol % taxol in liposomes; open squares: 1.6 mol % taxol in liposomes. (B) Lipid order parameter (S_{DPH}) calculated for liver basolateral membranes. The protein concentration was 0.1 mg/mL. Filled circles, BLM without taxol; filled squares, 0.2 mM taxol; open squares, 0.4 mM taxol.

(Figure 5A), consistent with the localization of taxol in the hydrophobic core of the bilayer. The calculated lipid order parameter (S) shows that 1 mol % taxol (with respect to lipid) decreases the order parameter of gel-state DPPC bilayers by approximately 17%. In the gel phase, the lipid molecules are packed in an all-trans conformation that restricts their motion. The factor S is a measure of lipid packing in the bilayer and can be defined as the reciprocal of fluidity (Van Blitterwijh et al., 1981). The observed decrease in the order parameter suggests that taxol induces a fluidizing effect in the gel phase of pure lipid bilayers, by affecting the packing of the acyl-chain domain of the membrane. Such an effect on membrane fluidity was observed previously for tamoxifen, a nonsteroidal anti-estrogen used in the treatment of cancer (Custodio et al., 1993); tamoxifen fluidizes the gel-phase DPPC bilayer, and the effect is believed to contribute to cytotoxicity recently observed for tamoxifen.

The incorporation of taxol also exerted a fluidizing effect on naturally occurring biological membranes. Vesicles derived predominantly from the basolateral plasma membrane of rat liver were labeled with DPH, and taxol was added from a

concentrated methanolic solution. DPH polarization was measured as a function of temperature and taxol concentration in the bilayer (Figure 5B). The lipid order parameter of the membrane vesicles decreased with increasing taxol concentration, suggesting a fluidizing effect of taxol. The effect most likely arises from incorporation of drug into the acyl-chain portion of the membrane. As a control for direct interaction of DPH with taxol, the emission spectra of DPH in tetrahydrofuran or in chloroform did not change upon addition of taxol. Therefore, the likelihood is low for probe quenching or direct interaction with taxol. Analysis by differential scanning calorimetry (DSC; described below) supports the conclusion that the effect of taxol on the probe polarization is through alteration of bulk membrane physical properties, rather than by the direct interaction of DPH and taxol.

X-ray Diffraction Studies. X-ray diffraction was used to probe for perturbation of the hydrocarbon chain region of DPPC vesicles by taxol. Information on the hydrocarbon chain conformation at temperatures below the gel-to-liquid-crystalline-phase transition can be extracted from the high-angle profile at 4.2 Å (Janiak et al., 1976). The high-angle region is characteristic of short-range ordering in the hydrocarbon chain packing. Pure DPPC vesicles showed a sharp reflection at 4.2 Å. With the incorporation of increasing mole fractions of taxol, the 4.2-Å reflection became more diffuse, suggesting that the incorporation of taxol affects the DPPC acyl chain conformation (data not shown). Such an effect is consistent with localization of taxol in the hydrophobic core of the bilayer.

Differential Scanning Calorimetric Studies. Given the effect of taxol on the acyl-chain domain of DPPC bilayers, the effects of drug on the phase transition of DPPC MLV were examined by differential scanning calorimetry, and the physical stability of the formulations was evaluated in parallel using optical microscopy. Panels A–C of Figure 6 show DSC thermograms of DPPC with increasing concentrations of taxol. Two thermal transitions were observed for DPPC vesicles in the absence of taxol (Figure 6A): a sharp acyl chain melting transition at 41.3 °C (313 °K) and small, broad pretransition at 36 °C (306 °K); these transitions correspond to those reported previously by others (Mabrey & Sturtevant, 1977).

Optical microscopy revealed that there was no drug precipitation from DPPC MLV containing 1 mol % taxol (Figure 6E); given the low aqueous solubility of taxol and the absence of an obvious precipitate, the majority of drug remained incorporated in the membrane. DSC showed that, with the incorporation of taxol at 1 mol %, the DPPC pretransition became undetectable (Figure 6B). The pretransition arises from the transformation from an L-β bilayer structure to the P-β conformation (Janiak et al., 1976). Because the pretransition is highly sensitive to the presence of other molecules in the polar region of the phospholipids, the loss of the pretransition cannot be ascribed to any specific molecular changes. In addition to the abolition of the pretransition, the sharp, highly cooperative main transition of DPPC liposomes was broadened, revealing a reduction in the cooperativity of the transition. The transition width at half-peak height ($T_{1/2}$) increased from 0.3 °C for pure DPPC to 0.5 °C for DPPC liposomes containing 1 mol % taxol. The main transition marks the transition of the bilayer from a highly hindered all-trans hydrocarbon chain conformation to a state in which some acyl chains exist in the gauche (kinked) conformation, resulting in greater phospholipid rotational freedom. The observed taxol-induced changes in the main phase transition supply further information on the hydrophobic location of the drug in the bilayer matrix. A broadening of

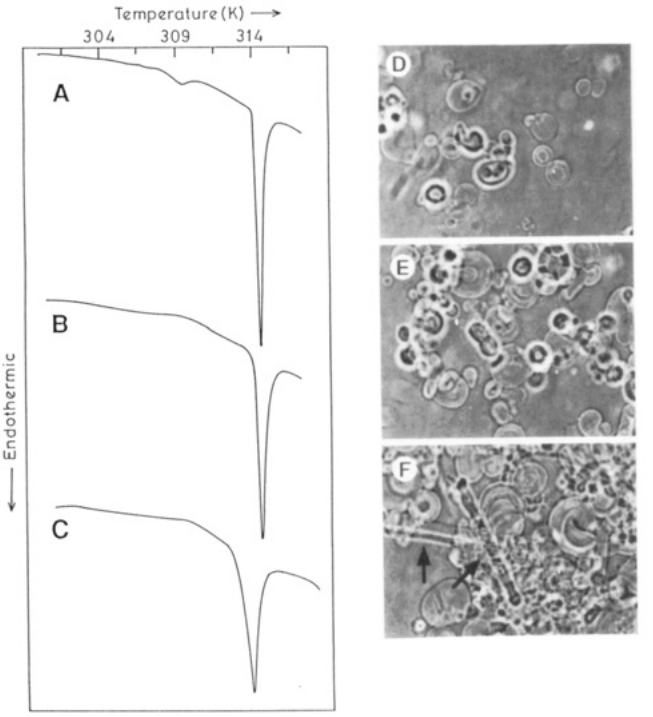

FIGURE 6: Effect of taxol concentration on the thermotropic behavior and physical stability of DPPC bilayer membranes. Multilamellar liposomes containing varying mole fractions of taxol were prepared from DPPC. Thermograms were acquired for samples using a scan rate of 2.5 °K/min, and parallel samples were observed by optical microscopy to detect precipitation of taxol. (A–C) Thermograms in the presence of (A) 0, (B) 1, and (C) 3 mol % taxol (with respect to lipid). (D–F) Phase contrast images of DPPC liposomes in the presence of (D) 0 mol % taxol, corresponding to (A); (E) 1 mol % taxol, corresponding to (B); and (F) 3 mol % taxol, corresponding to (C). Some taxol precipitates are visible in (F), appearing as needlelike crystals (arrows). The diameter of the liposomes was approximately 1–10 μm.

the main transition, without any change in the peak melting temperature, can be classified as an "A" type change (Jain & Wu, 1977); such effects would be expected if taxol were localized in the outer hydrophobic cooperative zone of the bilayer, i.e., in the region of the C1–C8 carbon atoms of the acyl chain. Such a location for taxol in the bilayer could be anticipated from the structure of the drug (Figure 1); the C13 side chain of taxol is relatively hydrophobic because of two aromatic rings, while the main taxane ring bears substituents (e.g., 7-OH and 9C=O) that have comparatively greater propensity for polar interactions.

As the concentration of taxol in lipid was increased to approximately 3 mol % (Figure 6B), the main transition broadened further, and the transition temperature was lowered by 0.4–0.6 °C. Thermograms taken during cooling also displayed similar main-transition broadening effects (data not shown). In the thermograms for higher taxol:lipid ratios, peak-broadening effects are observed together with small changes in the temperature axis. In parallel, light microscopy showed precipitation of taxol, as evidenced by needle-like taxol crystals (Figure 6F), suggesting that the changes observed by DSC in bilayer physical structure correlate with events accompanying destabilization of taxol:liposome formulations.

We hypothesize that at lower taxol:lipid ratios ($\leq$2 mol % for DPPC liposomes) the main transition broadens due to partitioning of taxol into the upper bilayer domain, toward the aqueous interface; such a localization results in the observed decrease in the cooperativity of the transition. At higher mole fractions of taxol, the main transition was both broadened and shifted, suggesting penetration of taxol deeper into the hydrophobic domain of the bilayer. Higher concentrations of

taxol in nonpolar solvents were observed by NMR and CD to undergo self-aggregation (cf. Figure 3A) (Balasubramanian et al., 1994). Increasing the mole fraction of taxol to ≥3 mol % results in self-aggregation of the drug within the bilayer, ultimately resulting in the appearance of distinct taxol domains and perhaps the nucleation of taxol precipitation that is observed macroscopically by optical microscopy (cf. Figure 6F). Evidence supporting taxol phase separation was observed clearly in thermograms of taxol–liposomes containing ≥6 mol % drug. At such high taxol concentrations, thermograms partly resemble the thermal characteristics of taxol-free DPPC liposomes (data not shown).

CONCLUSIONS

Several lines of evidence support the hypothesis that taxol incorporates into the hydrophobic domain of DPPC bilayer membranes and affects membrane physical properties such as the phase transition and the lipid order parameter or fluidity. Taxol incorporation is accompanied by conformational changes in the drug that involve both the C13 side chain and the main taxane ring, and by the appearance of higher-ordered structures such as taxol aggregates. The observed taxol-induced changes in liposomes may be important in understanding the factors that control both the maximal mole fraction of taxol that can be accommodated in the bilayer and the stability of such formulations during preparation, storage, and administration. In addition, since very little is known of the interaction of taxol or other taxanes with membranes, it is difficult at present to correlate structure with specific membrane-mediated cell functions. It is beyond the scope of existing knowledge to ascertain the relationship between the membrane-fluidizing effect of the anticancer drug taxol and the observation of altered membrane fluidity of cancer cells (Van Blitterwijh, 1984; Van Blitterwijh et al., 1981). Nonetheless, the biological ramifications of drug-induced changes in membrane physical properties are poorly elucidated and could be important contributors to the growing list of taxol effects on cell functions (Brugg & Matus, 1991; Ding et al., 1990).

ACKNOWLEDGMENT

We wish to thank Dr. M. Morris and Ms. Weihang Wang for providing rat liver basolateral plasma membrane vesicles; Dr. M. J. Levine of the Department of Oral Biology, SUNY/Buffalo School of Dental Medicine, for access to the Jasco CD; and Dr. W. Pangborn of the Medical Foundation of Buffalo for the X-ray diffraction data. We are grateful to Mr. Dan O'Connor of Hitachi, Inc. (Danbury, CT), for the loan of a Hitachi 1080 scanning fluorescence detector.

REFERENCES

Baker, J. K. (1992) *Spectrosc. Lett. 25*, 31–48.

Balasubramanian, S. V., Alderfer, J. L., & Straubinger, R. M. (1994) *J. Pharm. Sci.* (in press).

Blitzer, B. L., & Donovan, C. B. (1984) *J. Biol. Chem. 259*, 9295–9301.

Brugg, B., & Matus, A. (1991) *J. Cell Biol. 114*, 735–743.

Canaves, J. M., Ferragut, J. A., & Gonzalez-Ros, J. M. (1991) *Biochem. J. 279*, 413–418.

Chmurny, G. N., Hilton, B. D., Brobst, S., Look, S. A., Witherup, K. M., & Beutler, J. A. (1992) *J. Nat. Prod. 55*, 414–423.

Custodio, J. B. A., Almeida, L. M., & Madeira, V. M. C. (1993) *Biochim. Biophys. Acta 1150*, 123–129.

Deliconstantonos, G., Kopeikina-Tsiboukidou, L., & Villiotou, V. (1987) *Biochem. Pharmacol. 36*, 1153–1161.

Diamond, J. M., & Katz, Y. (1974) *J. Membr. Biol. 17*, 121–154.

Ding, A. H., Porter, F., Sanchez, E., & Nathan, F. C. (1990) *Science 248*, 370–372.

Donehower, R. C., Rowinsky, E. K., Grochow, L. B., Longnecker, S. M., & Ettinger, D. S. (1987) *Cancer Treat. Rep. 71*, 1171–1177.

Falzone, C. J., Benesi, A. J., & Lecomte, J. T. J. (1992) *Tetrahedron Lett. 33*, 1169–1172.

Grem, J. L., Tutsch, K. D., Simon, K. J., Alberti, D. B., Willson, E. V. K., Tormey, D. C., Swaminathan, S., & Trump, D. L. (1987) *Cancer Treat. Rep. 71*, 1179–1184.

Jain, M. K., & Wu, N. M. (1977) *J. Membr. Biol. 34*, 157–201.

Janiak, M. J., Small, D. M., & Shipley, G. G. (1976) *Biochemistry 15*, 4575–4580.

Kingston, D. G. I., Hawkins, D. R., & Ovington, L. J. (1982) *J. Nat. Prod. 45*, 466–470.

Lentz, R. B., Barenholz, Y., & Thompson, T. E. (1976) *Biochemistry 15*, 4521–4528.

Lorentz, M., Rieman, H. J., Schmal, A., Schult, H., Lang, S., Ohmann, C., Weber, D., Kapp, B., Luben, L., & Doenicke, A. (1977) *Agents Actions 7*, 63–67.

Mabrey, S., & Sturtevant, J. M. (1977) *Biochim. Biophys. Acta 486*, 444–450.

Mathew, A. E., Mejillano, M. R., Nath, J. P., Himes, R. H., & Stella, V. J. (1992) *J. Med. Chem. 35*, 145–151.

Popescu, M. C., Swenson, C. E., & Ginsberg, R. S. (1987) in *Liposomes—From Biophysics To Therapeutics* (Ostro, M. J., Ed.) pp 219–251, Marcel Dekker, New York.

Pottel, H., Van Der Meer, W., & Herreman, W. (1983) *Biochim. Biophys. Acta 730*, 181–186.

Ringel, I., & Horwitz, S. B. (1991) *J. Natl. Cancer Inst. 83*, 288–291.

Rowinsky, E. K., Cazenave, L. A., & Donehower, R. C. (1990) *J. Natl. Cancer Inst. 82*, 1247–1259.

Sarkar, S. N., Balasubramanian, S. V., & Sikdar, S. K. (1993) *Biochim. Biophys. Acta 1147*, 137–142.

Sharma, A., & Straubinger, R. M. (1994) *Pharm. Res. 11*, 889–896.

Sharma, A., Mayhew, E., & Straubinger, R. M. (1993) *Cancer Res. 53*, 5877–5881.

Shinitzky, M., & Barenholz, Y. (1978) *Biochim. Biophys. Acta 515*, 367–394.

Shinitzky, M., Dianoux, A. C., Gitler, C., & Weber, G. (1971) *Biochemistry 10*, 2106–2113.

Straubinger, R. M., Sharma, A., Murray, M., & Mayhew, E. (1993) *NCI Monogr. 15*, 69–78.

Swindell, C. S., & Krauss, N. E. (1991) *J. Med. Chem. 34*, 1176–1184.

Szoka, F. C., Jr. (1991) in *Membrane Fusion* (Wilschut, J., & Hoekstra, D., Eds.) pp 845–890, Marcel Dekker, New York.

Van Blitterwijh, W. J. (1984) in *Physiology Of Membrane Fluidity* (Shinitzky, M., Ed.) pp 53–83, CRC Press, Boca Raton, FL.

Van Blitterwijh, W. J., Van Hoeven, R. P., & Van Der Meer, B. W. (1981) *Biochim. Biophys. Acta 644*, 323–332.

Vander Velde, D. G., Georg, G. I., Gruewald, G. L., Gunn, C. W., & Mitscher, L. A. (1993) *J. Am. Chem. Soc. 115*, 11650–11651.

Wani, M. C., Taylor, H. L., Wall, M. E., Coggon, P., & McPhail, A. T. (1971) *J. Am. Chem. Soc. 93*, 2325–2327.

Williams, H. J., Scott, A. I., Dieden, R. A., Swindell, C. S., Chirlian, L. E., Francl, M. M., Heerding, J. M., & Krauss, N. E. (1993) *Tetrahedron 49*, 6545–6560.

Wright, S. E., & White, J. C. (1986) *Biochim. Biophys. Acta 863*, 297–304.